

Quantitative Measurements of Liquid Holdup and Drainage in Foam Using NMRI

Paul Stevenson

Centre for Multiphase Processes, University of Newcastle, Callaghan, NSW 2308, Australia

Michael D. Mantle, Andrew J. Sederman, and Lynn F. Gladden

Dept. of Chemical Engineering, University of Cambridge, Cambridge, CB2 3RA, United Kingdom

DOI 10.1002/aic.11068

Published online December 19, 2006 in Wiley InterScience (www.interscience.wiley.com).

Liquid fraction profiles of a column of draining aqueous foam stabilized with sodium dodecyl sulfate were studied by nuclear magnetic resonance imaging (NMRI) at high spatial and temporal resolution. It was observed that the liquid holdup in the column is not locally homogeneous in the direction of the column axis with liquid holdup exhibiting periodic variation in time. This creates "ripples" in the liquid content profiles (that is, an approximately sinusoidal variation of liquid fraction in space). These ripples are seen to actually rise in the column as liquid drains down through the foam. This behavior may be explained by a simple mass balance: the rising velocity of the ripples multiplied by the gas fraction in the foam is equivalent to the liquid superficial drainage rate. Thus, NMRI is proposed as a powerful tool for studying drainage of foams because it provides a noninvasive method of measuring superficial drainage rate in foams that yields time-resolved instantaneous drainage rates as a function of position in the column. The measured liquid drainage rates were compared with a dimensionless expression for the liquid drainage rate and excellent agreement was achieved.

© 2006 American Institute of Chemical Engineers *AIChE J.* 53: 290–296, 2007

Keywords: magnetic resonance imaging, foam, multiphase flow, fluid mechanics

Introduction

There are a number of techniques that can be used to measure the evolution of the volumetric liquid fraction (ϵ) within foam as drainage occurs. The measurement of capacitance or conductance of the foam is a common technique and its main advantage is that it is noninvasive.¹ However, it is difficult to achieve good spatial resolution and the inference of drainage rates from profiles of liquid volume fraction can be problematical. Nuclear magnetic resonance imaging (NMRI) methods can obtain the liquid holdup profile in a column of foam with excellent temporal and spatial resolution. Some of the earliest investigators of foam drainage using NMRI were Assink et al.,² who reported five drainage profiles of a small

column (1.13 cm in height) of aqueous foam stabilized with polymer and alcohol additives at up to 90 min after the foam was created. The one-dimensional (1D) NMRI results were qualitatively compared to a simple foam drainage model and showed poor agreement at short drainage times, although this improved for longer drainage times (typically 50 min). In a similar study, McCarthy³ examined the variation in proton signal intensity of egg white foams to follow the change in foam density with time using 1D magnetic resonance profile imaging. In addition, McCarthy examined how the spin–spin (T_2) relaxation behavior of the system varied with time and found that there were two distinct environments for the hydrogen nuclei of a draining foam: one corresponding to bulk-like liquid, predominantly in the Plateau borders, and the other being those adjacent to the gas–liquid interface of the foam. Since then only a few articles have been published

Correspondence concerning this article should be addressed to P. Stevenson at paul.stevenson@newcastle.edu.au.

in the literature addressing more general aspects of foam behavior. Gonatas et al.⁴ used two-dimensional NMRI to observe the coarsening inside a foam with time, whereas Prause et al.⁵ presented the first three-dimensional images of a gelatin solution foam; gelatin was chosen because drainage rates were slow, thus allowing for large acquisition time. None of these studies gave true quantitative measurement of either (1) liquid volume fraction during foam drainage or (2) the evolution of the local superficial liquid drainage velocity with increasing time.

Fully quantitative liquid holdup profiles of the free drainage of a column of aqueous foam are reported herein. High-spatial and temporal-resolution NMRI data were obtained (312 μm and 2 s, respectively) for the acquisition of foam liquid holdup profiles. Although downward drainage was observed as the liquid percolated through the froth, pockets of relatively high liquid holdup foam were seen to actually rise up the column in what we describe as *ripples*. When the position of these ripples is plotted as a function of time, the gradient of the monotonically rising curves that are apparent is equal to the (rising) velocity of the ripples in the foam. This seemingly curious phenomenon of rising ripples in draining foams will be explained by a simple mass balance on the foam. Moreover, the gradient of the ripples multiplied by the gas fraction will be shown to be equal to the local superficial liquid drainage velocity. Thus, for the first time, a new noninvasive method of directly measuring the free liquid drainage rate in foam systems is demonstrated at any point along the axis of the foam. In addition we show that the measured liquid drainage rate from foams stabilized with sodium dodecyl sulfate (SDS) is in excellent agreement with a simple dimensionless expression that correlates the nondimensionalized drainage rate with a power-law function of the volumetric liquid fraction.

The characterization of liquid drainage rate from foam is important not only to gain understanding of the behavior of stationary gas-liquid foams, but also to assist in prediction of the hydrodynamic condition of pneumatic froths in minerals flotation and foam fractionation.⁶ Neethling et al.⁷ asserted that two adjustable constants are required to characterize liquid drainage from foam to account for viscous losses within the Plateau borders and within the nodes, and they performed “forced drainage” experiments to ascertain their values for two different types of surfactant. The forced drainage experiments proceed by the formation of a very dry stationary foam, to which liquid at a known rate is added to the top surface. A “wet front” travels down the column of foam and, if the velocity of this front is measured, then the liquid drainage rate as a function of liquid holdup can be measured and therefore the values of the two necessary adjustable constants can be inferred. However, the forced drainage experiment can be problematic because the wet front velocity must be measured either visually, which is difficult and subjective, or by electrical tomographical methods, which require dedicated experimental apparatus. The technique described herein is presented as an alternative method of accurately measuring and characterizing liquid drainage rate in gas-liquid foam. NMRI’s specific advantages over other techniques are that it is a completely noninvasive and quantitative technique that allows the measurement of high spatial and temporal liquid holdups, providing information that is not available by other

techniques. These are done in situ without the addition of a tracer or further liquid and thus may be carried out without disturbing the measurement.

Experimental Technique

Two aqueous foams that were stabilized by SDS at 20% above the critical micelle concentration (that is, 2.92 g/L) were created: one was in solution with deionized water and the other viscosified with 40% v/v glycerol. Air was sparged through a glass frit at nominal superficial flow rates (see Table 1) into a pool reservoir of liquid at the base of a Perspex[®] (Plexiglas[®]) tube of internal diameter 47.7 mm. A hydraulic foam formed above the reservoir of liquid and was allowed to rise through the column for nearly 7 min, after which the air supply was switched off and data acquisition commenced. A section of the column located about 350 mm above the liquid-foam interface was scanned. Physical properties of the liquids as well as harmonic and arithmetic mean bubble sizes, determined by analysis of digital photographs of the foam using Optimas[®] image-analysis software (Optimas, Inc., Santa Clara, CA), are given in Table 1. The harmonic mean size, which is very close to the arithmetic mean, will be used in the following analysis for reasons previously discussed.⁸ Note that the photographs used to size the bubbles were taken on a run performed after the column had been removed from the spectrometer. Thus it cannot be claimed with certainty that bubble sizes representative of each run were measured. Three “sets” of experiments were performed; a *set* refers to experiments in which the physical properties of the liquid and the nominal air sparging rate to create the foam were kept constant. There were three individual runs in each set. However, because of difficulties in the precise control of the air rate, and given that liquid holdup in a foam is sensitive to the flow rate of gas used to create it, the liquid holdup at which the drainage profiles begin are not constant within a set. Experimental error on the measurement of the air rate is estimated at roughly 10%.

The NMRI experiments were performed on a Bruker DMX 200 spectrometer (Bruker Instruments, Billerica, MA), operating at a proton (¹H) frequency of 199.7 MHz. A 63-mm diameter birdcage radio frequency (RF) coil was used to excite and detect the NMR signal. Spatial resolution was achieved using a three-axis shielded gradient system capable of producing a maximum gradient strength of 0.139 T m⁻¹. The pulse sequence used to acquire the profiles was based on a standard 1D spin-echo profiling sequence.⁹ The raw signal intensity was corrected for spin-lattice (*T*₁) relaxation losses.

Table 1. Solution Properties and Mean Bubble Sizes

	Set 1	Set 2	Set 3
Nominal gas sparging rate (mm/s)	5.6	2.3	5.6
Dynamic viscosity (mPa·s)	4.0	4.0	1.0
Density (kg m ⁻³)	1104	1104	1000
Sample size	170	123	138
Arithmetic mean bubble diameter (mm)	0.82	0.82	0.58
Harmonic mean bubble diameter (mm)	0.81	0.80	0.58

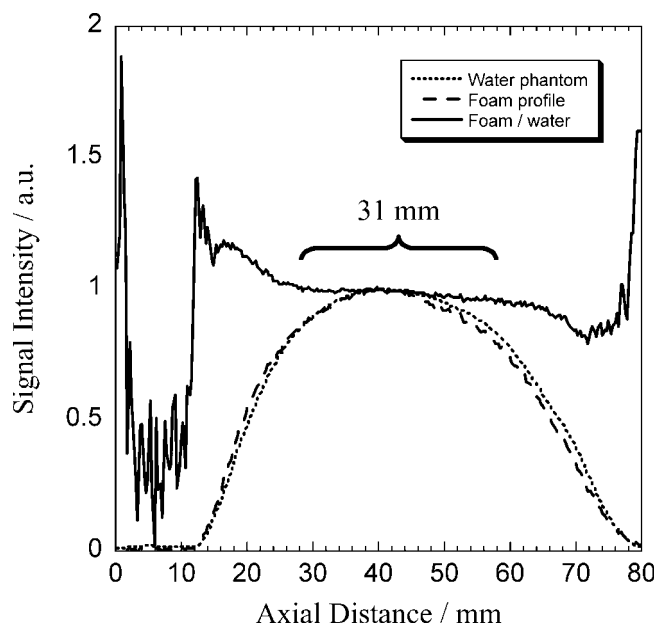


Figure 1. ^1H spin density profile of a water phantom, foam drainage data, and the result of RF homogeneity correction after division of the foam drainage data by the water phantom.

The solid line represents the result from division of the foam profile by the water phantom profile.

In addition, spin-spin (T_2) relaxation losses were also determined to be negligible at $<2\%$. The echo time (TE) and relaxation time (TR) for all experiments were 4.54 ms and 2.0 s, respectively; 256 complex data points were acquired over an axial field of view of 80.0 mm, thus giving a spatial resolution of 312 μm . A single scan profile was acquired every 2 s for typically >10 min.

A calibration phantom, to fully quantify the NMRI signal intensity, was prepared by mixing distilled water (H_2O) with heavy water (D_2O , Aldrich 99%) such that the volumetric water (H_2O) fraction was 0.1. The response of the phantom was measured and used to calculate a calibration factor so that the raw magnetic resonance data could be expressed as volumetric liquid fraction. In addition, this phantom was also used to correct for RF inhomogeneities of the excitation B_1 field following the method previously described.² The liquid holdup intensity profiles after RF homogeneity correction (performed by dividing every experimental liquid holdup profile by that of the water calibration phantom) showed that only 31 mm of the scanned 80 mm was found to be within 5% of unity (see Figure 1). Thus only sections 31 mm long are shown in the following results.

Results and Discussion

Liquid holdup profiles for one experiment in “Set 1” are shown in Figure 2. It is seen that the liquid fraction is approximately constant over the 31 mm of the column scanned and that drainage rate slows as the experiment progresses. Capillarity effects may be discounted in the modeling of drainage in this section because capillary forces are

absent if the holdup is macroscopically spatially invariant. However, even though it is seen that liquid fraction is *macroscopically* constant, it is not *locally* constant. For the data at zero seconds, a slight ripple, which is above the inherent noise level of the data, can be detected in the profile; this has a spatial wavelength of about 1.2 mm, which is roughly 50% greater than the harmonic mean bubble diameter (see Table 1). This arises from the geometric structure of the foam. Foam has a periodic structure made up of four Plateau borders that meet at a vertex (node), with very thin films or lamellae connecting the Plateau borders. It is reasonable to assert that when the liquid holdup in a thin slice is measured in a tube of finite cross-sectional area, the periodicity of the foam structure will cause some slices to exhibit higher liquid fraction than that of others because of the cellular nature of the froth structure. Similar ripples are seen in the relative fluid content vs. fluid height plot of Prause et al.⁵ The behavior of these *ripples*, with time, will be used here to directly determine liquid drainage rate in the foam.

The evolution of the average liquid holdup in the 31-mm section of the foam is shown in Figure 3 for all nine experiments. Note that the starting values of holdup differ within each set. Liquid holdup is strongly dependent on the gas flow rate used to form the foam.⁸ In the experiments described here the gas rate could not be controlled with precision, as described above; the reported gas rates should be considered nominal values only. Initial liquid holdup is highest for the runs in Set 1 because the highest gas rate was used and the elevated viscosity caused more liquid entrainment into the foam. Despite this, the liquid fraction converges to similar values as those seen in Set 2 that were for the same solution. Set 3 drains to lower values of liquid volume fraction because the viscosity of the interstitial fluid is lower.

The ripples discussed above obtained for one of the experiments in Set 1 are shown in Figure 4. Here, the first derivative with respect to time of the acquired signal is plotted on a time vs. axial height plot. The first derivative in time is plotted, rather than the absolute value of the signal, to improve visual contrast. The bright regions (positive difference value) in Figure 4 correspond to an increase in signal with respect to time and dark regions (negative difference

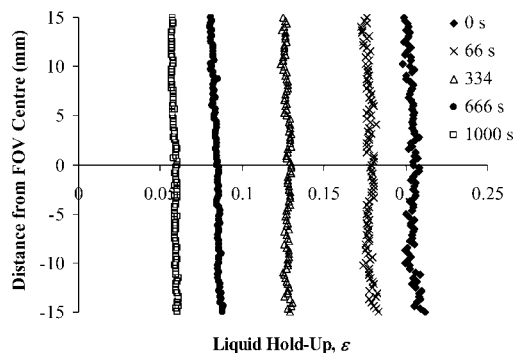


Figure 2. Liquid holdup profiles for one experiment in “Set 1.”

The extent of the data shown here is the region identified in braces in Figure 1.

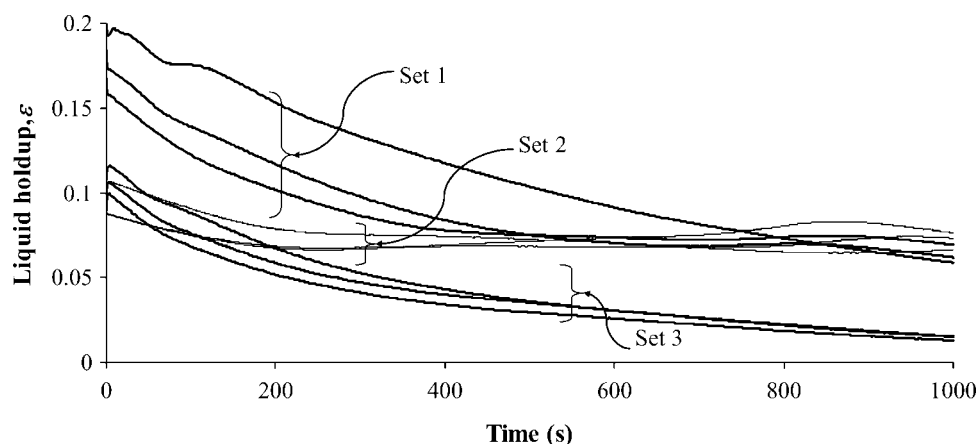


Figure 3. Time evolution of average liquid holdup.

value) correspond to a decrease in signal with respect to time. These ripples are seen to actually rise up the column as liquid drains down. This apparently counterintuitive behavior will be used to directly determine the drainage rate in foam and is explained in the next section. To obtain the ripple rise velocities from the magnetic resonance intensity profiles, a cross-correlation algorithm to automatically determine the gradient of the ripples in Figure 4 (and the other eight experiments) as a function of time was used. The cross-correlation is defined as

$$c(d) = \sum_i [x(i) * y(i + d)] \quad (1)$$

where $c(d)$ is the correlation at a shift of d (in this case a position shift) and $x(i)$ and $y(i)$ are two profiles (at a known time increment) to be compared. $c(d)$ is computed for all delays and the maximum in the correlation indicates the positional shift of the structural characteristics (ripples) in the profiles. Because the minimum shift that can be registered is one digital point, the raw data were first zero filled to 2048 complex points before Fourier transformation to improve the velocity resolution and to enable the identifica-

tion of smaller velocities. The velocity resolution is found by dividing the spatial resolution (here $39 \mu\text{m}$) by the time delay between the correlated profiles; herein a minimum velocity resolution was $2 \mu\text{m s}^{-1}$ and the maximum was $20 \mu\text{m s}^{-1}$. The profiles were B_1 corrected and normalized before cross-correlation so that the correlation of just the local intensity variations (ripples) were identified. For “Set 2” a further subtraction of neighboring profiles was necessary to remove slight global intensity variations arising from the very low intensity difference of the ripples, which were typically a fraction of <0.005 of the signal intensity and, individually, below the noise level of the profiles.

Slope of ripples used to calculate drainage rate

The *rising ripples* observed are explained by the fact that the liquid volume fraction in the foam is not locally constant because of the foam structure and, as liquid drains through the foam, gas bubbles must be displaced upward. Thus, in the absence of bubble breakage, the entire structure of the foam must rise in the column to allow for gas displacement. The velocity of the displaced foam is observed to be equal to the gradient of the ripples in Figure 4. To mathematically simulate this behavior the following model is adopted.

Consider the differential control volume shown in Figure 5. Making the assumption that both the gas and liquid phases are incompressible, a mass balance gives

$$\frac{dj_d}{dx} = (1 - \varepsilon) \frac{dV}{dx} - V \frac{d\varepsilon}{dx} \quad (2)$$

where V is the absolute velocity of the foam structure, x is the vertical length scale in the column, and j_d is the superficial liquid drainage rate. This can be simplified to

$$\frac{dj_d}{dx} = \frac{d[V(1 - \varepsilon)]}{dx} \quad (3)$$

Integrating Eq. 3 gives

$$j_d = V(1 - \varepsilon) + K \quad (4)$$

where K is a constant of integration and is readily seen to take the value of zero by considering an equilibrium froth with no drainage. Thus the velocity of the gas (foam structure, or the gradient of the ripples in Figure 4) multiplied by the volumetric gas fraction in the foam is seen to be identical to the

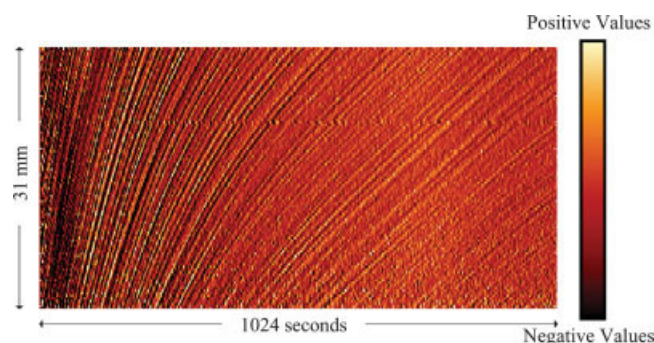


Figure 4. First derivative of arbitrary signal intensity with respect to time of one experiment in “Set 1.”

The first derivative is presented rather than the signal intensity itself to improve contrast and thus the clarity of the ripples. [Color figure can be viewed in the online issue, which is available at www.interscience.wiley.com.]

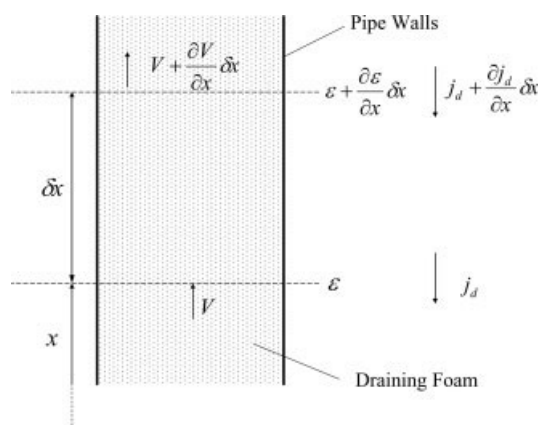


Figure 5. Control volume for a differential element of a draining foam.

superficial liquid drainage rate and is plotted in Figures 6–8. If the foam is to retain its structural identity (that is, there is no bursting of bubbles and Ostwald ripening is discounted) the absolute gas velocity must be equal to the velocity of the foam structure because the gas can only be displaced upward by traveling within a single bubble.

The method of experimentally determining liquid drainage rate is very accurate because we estimate that ε can be measured to within about 2% (the accuracy is governed by the accuracy of the D₂O calibration) and determination of the slope of the ripples is associated with only very few sources of error.

Calculated foam drainage rate

It was previously shown¹⁰ by dimensional analysis that, if inertial pressure losses were assumed to be negligible, the liquid superficial drainage rate expressed as a dimensionless Stokes-type number (Sk), where

$$Sk = \frac{j_d v}{g r_b^2} \quad (5)$$

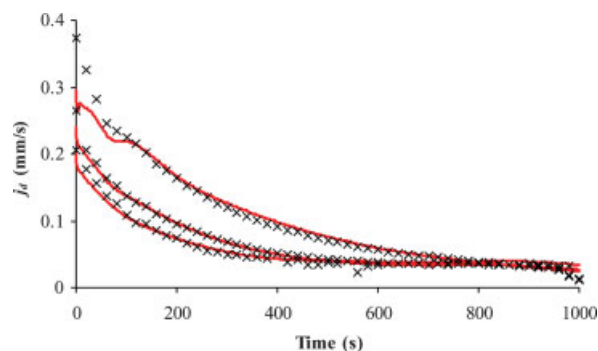


Figure 6. Experimentally measured drainage rate (crosses) and that calculated using Eq. 12 for the three experiments of "Set 1."

The calculated values are for the most part obscured by the experimental results. [Color figure can be viewed in the online issue, which is available at www.interscience.wiley.com.]

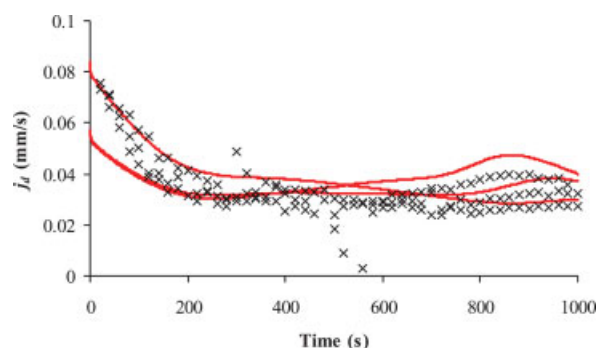


Figure 7. Experimentally measured drainage rate (crosses) and that calculated using Eq. 12 for the three experiments of "Set 2."

[Color figure can be viewed in the online issue, which is available at www.interscience.wiley.com.]

can be described by a function of ε only, that is,

$$Sk = f(\varepsilon) \quad (6)$$

Here, g is the acceleration due to gravity, r_b is the harmonic mean bubble radius, and v is the kinematic viscosity of the interstitial liquid.

In fact, a power-law relationship is seen to provide a remarkable fit to both existing experimental data and theoretical models, that is,

$$Sk = m \varepsilon^n \quad (7)$$

where m and n are dimensionless adjustable constants that implicitly contain information about the surface shear viscosity of the air–liquid interface and the viscous losses at the nodes in the foam where four Plateau borders meet. In fact, because an intrinsic factor such as shear viscosity is not measurable for systems with soluble surfactants,¹¹ and viscous losses within nodes are not, as yet, quantifiable, two adjustable constants are the minimum required to describe this system.

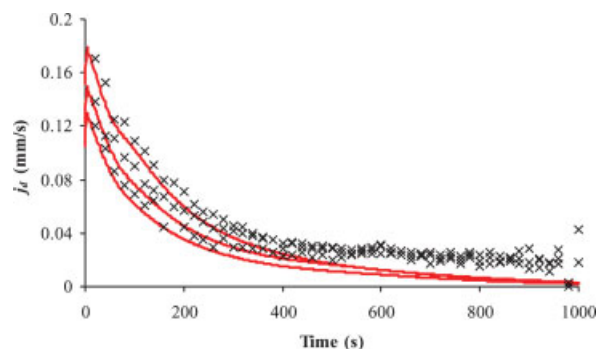


Figure 8. Experimentally measured drainage rate (crosses) and that calculated using Eq. 12 for the three experiments of "Set 3."

[Color figure can be viewed in the online issue, which is available at www.interscience.wiley.com.]

The Leonard–Lemlich model¹² for the drainage of foam, in which viscous losses are assumed to occur wholly within the Plateau borders, is shown⁹ to be approximated by

$$Sk = 0.0018\varepsilon^{1.92} \quad (8)$$

when the surface shear viscosity is assumed to be infinite (that is, the Plateau border walls are assumed to be rigid), whereas the model of Koehler et al.¹³ is well approximated by

$$Sk = \frac{0.49}{I} \varepsilon^{1.55} \quad (9)$$

which assumed that viscous losses occur only in the nodes of the foam rather than in the Plateau borders, where I is the same dimensionless adjustable constant used by Koehler et al.¹³ In addition Stevenson¹⁰ showed that the drainage data of Neethling et al.⁷ fit

$$Sk = 0.012\varepsilon^{1.74} \quad (10)$$

for foams stabilized by SDS and

$$Sk = 0.013\varepsilon^{1.78} \quad (11)$$

for foams stabilized by tetradecyltrimethyl ammonium bromide (TTAB) at undisclosed concentrations. The rigid-walled Leonard–Lemlich model (represented by Eq. 8) underpredicts the drainage rate experimentally measured by Neethling et al. by a factor of about 10 because the Plateau border walls, in practice, exhibit surface mobility. The semiempirical model of Koehler et al.¹³ is only in moderate agreement with the experimental data, even after the adjustable constant I has been fitted, because of the constraint that there are no viscous losses in the Plateau borders (that is, zero surface shear viscosity).

Note that capillarity effects can be discounted in this work because the data shown in Figure 2 are essentially invariant in height.

Comparison of measured and calculated drainage rates

In Figure 6 it is seen that, on a plot against liquid superficial drainage rate j_d vs. time that Eq. 7 gives excellent agreement to the data of “Set 1” with values of m and n such that

$$Sk = 0.016\varepsilon^2 \quad (12)$$

These constants are close to those that fit previously reported data⁷ (Eq. 10) for foams stabilized with SDS, obtained using the method of forced drainage. However, surface shear viscosity (and therefore m and n) changes with surfactant concentration; Neethling et al.¹³ do not disclose the surfactant concentration at which they worked. Note that the values of the adjustable constants used in Eq. 12 are only appropriate for the type and concentration of surfactant used in these experiments (that is, 2.92 g L⁻¹ SDS). The procedure must be repeated if the values of the constants that pertain to different surfactant systems are required. The agreement of Eq. 12 with the data of “Set 2” is reasonable, but less satisfactory than that of “Set 1” (see Figure 7). For the experiments of “Set 3,” Eq. 12 is in good agreement with the drainage

rate at a short time (Figure 8), although it significantly undercalculates (by a factor of roughly 5) the drainage rate at longer times when ε becomes small. It is suggested that the undercalculation of the actual flow rate may be explained by the bursting of bubbles within the foam, causing excess liquid drainage over and above that calculated by Eq. 12. Liquid associated with a bubble that bursts is liberated and drains downward. Quantification of the excess liquid drainage could provide an indirect method of determining bubble coalescence within the bulk of the froth.

Conclusions

(1) Nuclear magnetic resonance imaging scans of the free drainage of an aqueous foam stabilized with SDS were used to quantitatively ascertain the time evolution of liquid volume fraction in a foam.

(2) The scans reveal curious ripples of relatively high liquid fraction that rise in the column as liquid drains down. By introducing a dynamic volume balance, it was shown that the gradient of these ripples, plotted on a graph of height vs. time, multiplied by the volumetric gas fraction of the foam, is equivalent to the superficial drainage rate of the liquid. Thus the superficial liquid drainage rate from foam can be measured noninvasively.

(3) This experimentally measured drainage rate has been compared to a simple dimensionless expression (Eq. 12). The agreement is excellent for wet foams with more viscous interstitial liquid. Moreover, it appears that in experiments using a less viscous interstitial liquid, in which bubble breakage is expected to be greater, that the excess drainage resulting from bubble breakage may be ascertained for the difference between the actual total drainage rate and that calculated by Eq. 12 fitted to the data at earlier times in the experiment.

Acknowledgments

The support provided by an Australian Research Council Discovery-Projects grant is acknowledged. MDM, AJS, and LFG thank the EPSRC for provision of the MRI spectrometer. Dr. Robert Niven of the Australian Defence Force Academy gave useful comments on a draft of this manuscript and Miss Jacqueline Hicks performed the bubble sizing.

Notation

d = bubble diameter, m
 g = acceleration due to gravity, m s⁻²
 I = Koehler’s adjustable constant used in Eq. 9
 j_d = liquid superficial velocity, m s⁻¹
 K = a constant of integration, m s⁻¹
 r_b = bubble radius ($\equiv 0.5d$), m
 Sk = Stokes-type number defined in Eq. 5
 t = time, s
 V = absolute gas velocity, m s⁻¹
 x = vertical distance in the column (measured positive upward), m

Greek letters

ε = volumetric liquid fraction in the foam
 ν = liquid kinematic viscosity, m² s⁻¹

Literature Cited

1. Barigou M, Deshpande NS, Wiggers FN. An enhanced electrical resistance technique for foam drainage measurement. *Colloids Surf A*. 2001;189:237–246.
2. Assink RA, Caprihan A, Fukushima E. Density profiles of a draining foam by nuclear magnetic resonance imaging. *AIChE J*. 1988;34:2077–2079.
3. McCarthy MJ. Interpretation of the magnetic resonance imaging signal from a foam. *AIChE J*. 1990;36:287–290.
4. Gonatas CP, Leigh JS, Yodh AG, Glazier JA, Prause B. Magnetic resonance-images of coarsening inside a foam. *Phys Rev Lett*. 1995;75:573–576.
5. Prause BA, Glazier JA, Gravina SJ, Montegmagno CD. Three-dimensional magnetic resonance imaging of a liquid foam. *J Phys: Condens Matter*. 1995;7:511–515.
6. Stevenson P. The wetness of a rising foam. *Ind Eng Chem Res*. 2006;45:803–807.
7. Neethling SJ, Lee HT, Cilliers JJ. A foam drainage equation generalized for all liquid contents. *J Phys: Condens Matter*. 2002;14:331–342.
8. Stevenson P, Stevanov C. Effect of rheology and interfacial rigidity on liquid recovery from rising froth. *Ind Eng Chem Res*. 2004;43:6187–6194.
9. Callaghan PT. Principles of Nuclear Magnetic Resonance Spectroscopy. Oxford, UK: Clarendon Press; 1993.
10. Stevenson P. Dimensional analysis of foam drainage. *Chem Eng Sci*. 2006;61:4503–4510.
11. Stevenson P. Remarks on the shear viscosity of surfaces stabilised with soluble surfactants. *J Colloid Interface Sci*. 2005;290:603–606.
12. Leonard R, Lemlich R. A study of interstitial liquid flow in foam. *AIChE J*. 1965;11:18–25.
13. Koehler SA, Hilgenfeldt S, Stone HA. Liquid flow through aqueous foams: The node-dominated foam drainage equation. *Phys Rev Lett*. 1999;82:4232–4235.

Manuscript received Mar. 23, 2006, revision received Sept. 12, 2006, and final revision received Nov. 10, 2006.